

from the total microscopic field the self-field of the electron being excited, which does not contribute to the local field inducing the transition. As a result, they found $\epsilon_2^{\text{micro}} < \tilde{\epsilon}_2$ for lower ω , increasing the disparity between theory and experiment, which is to be expected. In fact, subtracting the self-field will enhance $\epsilon_2^{\text{micro}}$ over $\tilde{\epsilon}_2$ for lower ω and bring about closer agreement between theory and experiment. This is a result of the transformation in Eq. (1), as seen in Fig. 1, and even when there are ions at noncubic sites, we find $\epsilon_2^{\text{micro}} < \epsilon_2$ for low ω . Thus their hypothesis of significant dynamical correlation effects is unnecessary. Subtraction of the electron's self-field, a difficult problem, might be best accomplished by use of a phenomenological parameter, as suggested by Wiser.²

In summary, the influences of local-field effects in the optical spectra of solids must be kept in mind when the spectra are interpreted or used to evaluate theoretical calculations. An upper limit to the magnitude of local-field corrections is obtained from Eq. (1), while the degree of initial-state localization suggests what fraction of the full Lorentz local-field correction is appropriate.

We appreciate the encouragement and support of Professor H. Fritzsche.

*Work supported by the Wisconsin Alumni Research Foundation, and the U. S. Air Force Office of Scientific Research under Contract No. AFOSR-70-1943-Amendment A.

†Work supported by the U. S. Air Force Office of Scientific Research under Contracts No. F44620-71-C-0025 and No. F44620-70-C-0029, and the National Science Foundation.

¹See, e.g., F. Stern, in *Solid State Physics*, edited by F. Seitz and D. Turnbull (Academic, New York, 1963), Vol. 15, Sect. 24.

²N. Wiser, *Phys. Rev.* **129**, 62 (1963); S. L. Adler, *Phys. Rev.* **126**, 413 (1962).

^{3a}J. A. Van Vechten and R. M. Martin, *Phys. Rev. Lett.* **28**, 446 (1972).

^{3b}R. M. Martin *et al.*, *Phys. Rev. B* **6**, 2500 (1972).

⁴M. A. Graber, thesis, Princeton University, 1970 (unpublished).

⁵See, e.g., J. M. Ziman, *Principles of the Theory of Solids* (Cambridge Univ. Press, London, 1964), p. 229.

⁶G. W. Rubloff, *Phys. Rev. B* **5**, 662 (1972).

⁷M. L. Cohen and V. Heine, in *Solid State Physics*, edited by H. Ehrenreich, F. Seitz, and D. Turnbull (Academic, New York, 1970), Vol. 24, and references therein.

⁸J. P. Walter and M. L. Cohen, *Phys. Rev. B* **4**, 1877 (1971).

⁹Y. Onodera and Y. Toyozawa, *J. Phys. Soc. Jap.* **22**, 833 (1967).

¹⁰H. Saito, *Sci. Light (Tokyo)* **20**, 1 (1971).

¹¹J. C. Phillips, *Phys. Rev. Lett.* **12**, 447 (1964); K. P. Jain, *Phys. Rev.* **139**, A544 (1965).

¹²U. Fano, *Phys. Rev.* **124**, 1866 (1961).

Random-Phase-Approximation Correlation Energy in Metallic Hydrogen Using Hartree-Fock Bloch Functions*

Hendrik J. Monkhorst and Jens Oddershede†

Department of Physics, University of Utah, Salt Lake City, Utah 84112

(Received 22 January 1973)

Correlation energies for simple-cubic metallic hydrogen are calculated using random-phase-approximation (RPA) methods. Hartree-Fock Bloch functions for the real lattice, including those for excited bands, were used as zeroth-order states. About 60% of the RPA correlation energy originates from intraband excitations. The RPA correlation energy, including exchange, is estimated to be about -0.024 hartree/electron near the Hartree-Fock equilibrium, leading to a total energy of about -0.490 hartree/atom.

The treatment of electron correlation effects in real metals is still an outstanding problem. For the limiting cases of high and low electron densities satisfactory methods exist.^{1,2} The difficulties at intermediate densities arise since the kinetic energy and potential energy are comparable. This leads to the breakdown of the electron-gas model, particularly for the calculation of to-

tal energies, since the actual electron-lattice interactions are not negligible. But this implies that plane waves are no longer appropriate unperturbed functions in a perturbation treatment of the correlation problem. In this communication we present many-body theoretical results of correlation-energy calculations for simple-cubic metallic hydrogen using Hartree-Fock Bloch

(HFB) orbitals for lowest³ and excited bands as zeroth-order states. The major new physical effects thus taken into account are the exact (non-local) exchange term in the HFB orbital energies and the band gaps at the first Brillouin zone (BZ) boundary. Since the electron-lattice interaction is treated correctly in the HF calculations, we also get a realistic total energy. This approach was suggested by the success of perturbation calculations on atoms starting from HF results.⁴

The HF model does not account for any long-range screening effects. Therefore, random-phase-approximation (RPA) methods should be used to overcome the divergencies in all but the first order of perturbation. It is generally argued that the RPA is invalid at intermediate densities. However, it should be recalled that, as in any incomplete perturbation treatment, the convergence towards the correct answer depends heavily on the choice of unperturbed states. The conventional RPA-like formulation invariably starts from the electron-gas model which, as pointed out above, is an unrealistic starting point. We shall here report on preliminary numerical results which indicate that our application of RPA accounts for a major part of the correlation energy.

RPA correlation energies were obtained by summing ring diagrams. Also exchange diagrams were evaluated. In this Letter we only briefly comment on the methods used. A more complete report will be published elsewhere.

Consider a simple-cubic crystal at 0°K and with lattice spacing a , built up from N hydrogen atoms. Let $\epsilon_m(\vec{k})$ and $|\vec{k}m\rangle$ be the HFB energy and spin orbitals for the m th band, respectively. In the reduced-zone scheme the Bloch vectors \vec{k} are to be inside the first BZ. Here the lowest band ($m = 1$) is half-filled. The zeroth-order Hamiltonian of this system is the sum over the N HFB operators. With Bloch orbitals the only nonzero matrix elements for the associated perturbation Hamiltonian are the electron interaction integrals over HFB orbitals. Preparatory to later developments we introduce the approximation

$$\langle \vec{k}_1 i; \vec{k}_2 j | r_{12}^{-1} | \vec{k}_1 + \vec{q}, m; \vec{k}_2 - \vec{q}, n \rangle \approx v_{i,j,mn}(\vec{q}). \quad (1)$$

We found this to be particularly valid when $i = j = m = n = 1$ (intra-band matrix elements). It is reasonably good when $i = j = 1$, m and/or $n \neq 1$ (inter-band matrix elements). Since i and j are always 1, we will suppress these indices.

With this assumption the multiband Dyson-like equation for the RPA can diagrammatically be ex-

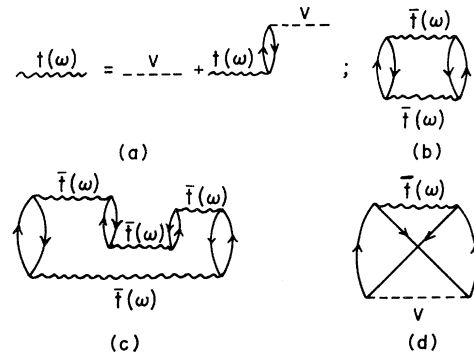


FIG. 1. Diagrammatic representation of some correlation contributions considered. (a) Dyson-like equation in the RPA. (b) Second-order diagram with screened interactions. (c) A diagram not included in (b). (d) Second-order exchange diagram with one screened interaction.

pressed as in Fig. 1(a), where $t(\omega)$ is the frequency-dependent ring propagator. We considered two solutions to that equation, namely the regular sum over all ring diagrams and a sum over ring diagrams with “forward” time ordering only [ring diagrams that at a certain time have only two hole (and particle) propagator lines]. This implies that diagrams like Fig. 1(c) are not included in this sum. In this case the Dyson-like equation gives for the lowest band ($i = j = m = n = 1$) a $\bar{t}(\omega)$ matrix element that can be expressed as a screened Coulomb interaction

$$\bar{t}_{11}(\vec{q}, \omega) = v_{11}(\vec{q}) / [1 + v_{11}(\vec{q}) \Lambda^2(\vec{q}, \omega)], \quad (2)$$

$$\Lambda^2(\vec{q}, \omega) = -\sum_{\vec{k}} [\omega + \omega_1(\vec{k})]^{-1}, \quad (3)$$

$$\omega_m(\vec{k}) = \epsilon_1(\vec{k}) - \epsilon_m(\vec{k} + \vec{q}), \quad (4)$$

where the \vec{k} sum is over hole states \vec{k} , for which $\vec{k} + \vec{q}$ are particle states within the first BZ. For forward-time ordering the RPA correlation energy can be expressed diagrammatically as in Fig. 1(b).

At this point it is of interest to notice that $\Lambda^2(\vec{q}, 0) \sim 1/\ln q$ as $\vec{q} \rightarrow 0$. This is because the exchange term in $\omega_1(\vec{k})$ vanishes like $q \ln q$ for small q and hence dominates over the kinetic-energy term which is linear in q . As a result of this property, \bar{t}_{11} diverges logarithmically for small q . This behavior is a typical result of a rigorous treatment of HF exchange,⁵ but this divergence is not strong enough to cause problems in the evaluation of correlation energies. The effective interaction in Eq. (2) was used to calculate exchange diagrams like the one depicted in Fig. 1(d).

When we allowed for all time ordering in the

Dyson-like equation, we obtained a correlation energy expression that is a generalization of the relation between the total energy and the imaginary part of the inverse dielectric function.⁶ Since we used HFB functions and energies, the dielectric function is related to the one derived by Ehrenreich and Cohen in the multiband case.⁷ Integrations were performed with Gaussian quadratures. All accuracies in these are about 1%.

In the initial calculation of correlation energy for metallic hydrogen only the lowest bands were taken into account. For $v_{11}(\vec{q})$ and $\omega_1(\vec{k})$ we used the HFB orbitals and energies obtained in earlier work.³ There we found that the Fermi surface is essentially spherical and that the occupied HFB orbitals can be well represented by

$$|\vec{k}1\rangle = \exp(2\pi i \vec{k} \cdot \vec{r}/a) \sum_{\vec{\mu}} \varphi_1(\vec{r} - a\vec{\mu}). \quad (5)$$

The sum is over the 1s Slater-type orbitals φ_1 centered at lattice points $a\vec{\mu}$. We assumed that the particle states in the first band could also be given by Eq. (5). As indicated below this proved to be a valid assumption.

In Table I we have collected some typical intraband results for correlation energies with all time ordering (ΔE) and forward time ordering ($\Delta \bar{E}$). We see that 60% to 70% of the RPA correlation energy is obtained with the forward-time propagator \bar{t}_{11} , the remaining part arising from "irregular" diagrams like the one depicted in Fig. 1(c). In Table I, column 3, we have given crude estimates of this diagram. These were obtained by averaging an upper and lower bound to this diagram. Since their values are a large fraction of $\Delta E - \Delta \bar{E}$ we conclude that considerable cancellation occurs among higher-order diagrams. With \bar{t}_{11} we can also study the effect of screening on the second-order exchange diagram. Data for unscreened and partially screened exchange [Fig.

1(d)] are also given. Screening does not reduce the exchange diagram very much. In addition we observe a relatively weak dependence on the lattice spacing a . This should be compared with the strict density independence when the kinetic-energy operator is used as zeroth-order Hamiltonian.¹

The $v_{11}(\vec{q})$ are expressed as reciprocal-lattice sums.³ We found that they could be approximated very well with only the first term. Actually ΔE and $\Delta \bar{E}$ increased only by about 1% when we included the lattice sum, the effect being larger for larger lattice spacings.

In the next series of calculations we estimated the effects of more realistic particle states in the lowest band and the effects of including excited bands in the calculation. We obtained excited band functions and energies as eigenvectors and eigenvalues of the HFB matrix over plane waves (PW's), using the previously obtained³ Fock operator. From the discrepancies between the band energies $\epsilon_1(\vec{k})$ obtained earlier and in this work, we inferred a few-percent distortion of the Fermi surface from its assumed spherical shape. If the PW-HF formulation as described above were carried to self-consistency, we estimate the effect on the HF energy to be about 1%. Currently, we are investigating this in more detail. In the PW-HF formulation we observed only a few-percent change in the v -matrix elements, but the particle energies were strongly affected near the BZ boundary. There the band energies are lowered considerably and their gradient in \vec{k} space now approaches zero. The interband matrix elements are clearly more dependent on (\vec{k}_1, \vec{k}_2) values. These quantities are a measure of the PW mixing due to the electron-lattice interaction. In the following calculations we invoked the approximation of Eq. (1) by evaluating v -matrix elements for a (\vec{k}_1, \vec{k}_2) pair taken roughly in the center of the allowed \vec{k} integration range, as in Eq. (3). This obviously is quite a crude approximation because of the strong PW mixing close to the BZ boundaries when m and/or $n \neq 1$. Numerical analysis has indicated that it causes roughly a 10% error in the interband excitation contributions to the RPA correlation energies.

In Table II we have given, for certain selected values of the lattice spacing a , the correlation energy per electron calculated by summing *all* ring diagrams. By comparing the ΔE values in Tables I and II, based on intraband excitations only, the effect of the use of realistic particle states in the lowest band can be observed. The

TABLE I. RPA correlation energies (in hartrees/electron) for various lattice spacings a (in bohrs), calculated with intraband excitations only. (1) Sum of ring diagrams with forward-time ordering only ($\Delta \bar{E}/N$). (2) Sum of all ring diagrams ($\Delta E/N$). (3) Estimated fourth-order-type diagram [see Fig. 1(c)]. (4) Second-order exchange diagram. (5) Same as (4), but with one screened interaction $\bar{t}_{11}(\omega)$ [see Fig. 1(d)].

a	(1)	(2)	(3)	(4)	(5)
3.50	-0.00856	-0.0131	-0.0025	0.0028	0.0022
2.73	-0.0104	-0.0156	-0.003	0.0031	0.0025
1.00	-0.0207	-0.0291	-0.006	0.0042	0.0037

TABLE II. RPA correlation energies $\Delta E/N$ calculated as a sum of *all* ring diagrams, including interband excitations and screened exchange diagram values. The estimated total correlation energy is compared with predictions from the Gell-Mann-Brueckner high-density formula (Ref. 1). Energies are in hartrees/electron, and lattice spacings a are in bohrs. (1)–(4) $\Delta E/N$ including contribution from 1 to 4 bands. (5) Screened exchange diagram [Fig. 1(c)], calculated with intraband excitations only. (6) Estimates of total correlation energy. (7) Correlation energies from high-density electron-gas formula (Ref. 1).

a	(1)	(2)	(3)	(4)	(5)	(6)	(7)
3.50	-0.018	-0.025	-0.026	-0.026	0.0044	-0.020	-0.0239
2.73	-0.020	-0.028	-0.029	-0.030	0.0044	-0.024	-0.0316
1.00	-0.035	-0.046	-0.047	-0.048	0.0053	-0.041	-0.0628

exchange diagram with one screened interaction is changed most drastically. This comes from the inherently large contribution to its value from large momentum transfer \vec{q} .

In Table II we have also given the results of ΔE calculations as an increasing number of excited bands are taken into account. These data indicate that 60% to 70% of the RPA correlation energy comes from intraband excitations and that the second band gives most of the interband contributions. For very small a values we should ultimately approach the high-density limit, in which interband excitations should be negligible. It is therefore consistent to find the proportionally largest intraband excitation contribution at the smallest lattice spacing.

In the last two columns of Table II we have compared tentative estimates of the total RPA correlation energy, including exchange, and the values from Gell-Mann and Brueckner's high-density electron-gas formula.¹ The estimates are made by adding ΔE from column 4 to the screened exchange value of column 5, increased by 30% to correct for excited band contributions. Though our numbers are still in error to about 10%, as a result of Eq. (1), the difference between the last two columns is significant. The high-density results are unrealistically large for all a , whereas our result for the value a near the HF minimum comes quite close to the expected -0.02 hartree/electron known from atoms and small molecules.⁸ Also our estimates exhibit a weaker dependence on a (or, equivalently, the electron density) than the Gell-Mann-Brueckner values

—again in accordance with experience from atomic and molecular calculations.⁸

Finally, we want to point out that the HF energy exhibits a minimum of about -0.466 hartree near $a = 2.73$ bohr.³ Hence the sum of the HF energy and RPA correlation energy is about -0.490 hartree, well above the free-atom value.

We are highly indebted to Dr. N. C. Dutta for many exciting discussions, to Dr. F. E. Harris for inspiration and support, to Dr. L. Kumar for computational assistance, and Dr. J. Linderberg for introducing us to the Green's-function formulation.

*Research sponsored in part by the U.S. Air Force Office of Scientific Research, Office of Aerospace Research, under Grant No. AFOSR-71-1992, and in part by the National Science Foundation under Grant No. GP-31373X.

†On leave from the Chemistry Department, University of Aarhus, Aarhus, Denmark.

¹M. Gell-Mann and K. A. Brueckner, Phys. Rev. **106**, 364 (1957).

²E. P. Wigner, Trans. Faraday Soc. **34**, 678 (1938).

³F. E. Harris, L. Kumar, and H. J. Monkhorst, Phys. Rev. B **7**, 2850 (1973).

⁴H. P. Kelly, Advan. Chem. Phys. **14**, 219 (1967).

⁵K. J. Duff and A. W. Overhauser, Phys. Rev. B **5**, 2799 (1972).

⁶L. Hedin and S. Lundquist, Solid State Phys. **23**, 75 (1969).

⁷H. Ehrenreich and M. H. Cohen, Phys. Rev. **115**, 786 (1959).

⁸E. Clementi, IBM J. Res. Develop. **9**, 2 (1965).